



Use of cardiac magnetic resonance to detect changes in metabolism in heart failure

William D. Watson¹, Jack J. J. Miller^{1,2,3}, Andrew Lewis¹, Stefan Neubauer¹, Damian Tyler^{1,2}, Oliver J. Rider¹, Ladislav Valkovič^{1,4}

¹Oxford Centre for Clinical Magnetic Resonance Research, ²Department of Physiology, Anatomy and Genetics, ³Department of Physics, Clarendon Laboratory, University of Oxford, Oxford, UK; ⁴Department of Imaging Methods, Institute of Measurement Science, Slovak Academy of Sciences, Bratislava, Slovakia

Contributions: (I) Conception and design: WD Watson, JJJ Miller, L Valkovič; (II) Administrative support: None; (III) Provision of study materials or patients: None; (IV) Collection and assembly of data: None; (V) Data analysis and interpretation: None; (VI) Manuscript writing: All authors; (VII) Final approval of manuscript: All authors.

Correspondence to: Dr. William D. Watson. Oxford Centre for Clinical Magnetic Resonance Research (OCMR), Level 0, John Radcliffe Hospital, Headington, Oxford OX3 9DU, UK. Email: william.watson@cardiov.ox.ac.uk.

Abstract: The heart has a massive adenosine triphosphate (ATP) requirement, produced from the oxidation of metabolic substrates such as fat and glucose. Magnetic resonance spectroscopy offers a unique opportunity to probe this biochemistry: ³¹Phosphorus spectroscopy can demonstrate the production of ATP and quantify levels of the transport molecule phosphocreatine while ¹³Carbon spectroscopy can demonstrate the metabolic fates of glucose in real time. These techniques allow the metabolic deficits in heart failure to be interrogated and can be a potential future clinical tool.

Keywords: Metabolism; cardiomyopathy; heart failure; magnetic resonance

Submitted Nov 19, 2019. Accepted for publication Dec 18, 2019.

doi: 10.21037/cdt.2019.12.13

View this article at: <http://dx.doi.org/10.21037/cdt.2019.12.13>

Introduction

The heart is an organ with a massive energy requirement: continuously active, it needs adenosine triphosphate (ATP) not just for contraction but also for relaxation and the movement of ions necessary to regulate this process. This ATP is in healthy heart formed primarily from the oxidation of fats (60–70%) and glucose (30–40%), although there is a small contribution from lactate, ketones and amino acids (1). Key to the heart's abilities is a flexibility to take advantage of the best fuel for the prevailing situation, for instance increasing glucose oxidation following insulin release or during conditions of ischaemia (2).

In the failing heart, rates of fat and glucose oxidation fall, flexibility is lost and ATP supply is impaired (3). This is seen irrespective of cause and has raised interesting questions about how the heart responds to insults and transitions into a failure state from the metabolic perspective.

Magnetic resonance of the heart offers an exciting ability to measure these changes non-invasively. Hydrogen (¹H), Phosphorus (³¹P) and Carbon (¹³C) spectroscopy all offer different perspectives to examine biochemical processes within the myocardium, for example, ³¹P spectroscopy determines the relative proportion of ATP and its energy reserve phosphocreatine (PCr). These MRS techniques have long formed a tool that allows us to uncover metabolic changes *in vivo* noninvasively.

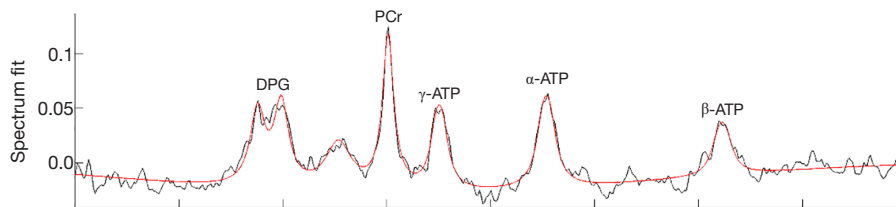
Use of high field strength MR scanners in recent years has increasingly allowed these to be detected with better spatial and temporal resolution, allowing spectra to be better localised to the heart and seen with greater clarity for more information.

Principles of spectroscopy in CMR

Conventional cardiac magnetic resonance imaging is reliant

Table 1 Elements studied with MRS and their potential applications

MR element	Metabolic pathways/cellular biochemistry	Applications
Phosphorus (^{31}P)	ATP synthesis; ATP transfer via Phosphocreatine; pH	Conditions where energy supply is disrupted in a global fashion, such as dilated cardiomyopathy, diabetes or valvular heart disease
Carbon (^{13}C)	Glucose metabolism (pyruvate dehydrogenase); Krebs cycle; fatty acid metabolism	Conditions where there are metabolic abnormalities such as dilated cardiomyopathy, diabetes, obesity or ischaemic heart disease
Hydrogen (^1H)	Triglyceride; creatine	Conditions where there is abnormal storage of fat within the myocytes, such as obesity or diabetes. Disruption of the creatine pool in dilated cardiomyopathy
Deuterium (^2H)	Yet to be studied but in theory glucose or fat metabolism	Conditions where there are metabolic abnormalities such as dilated cardiomyopathy, diabetes, obesity or ischaemic heart disease
Sodium (^{23}Na)	Intracellular sodium currents	Myocardial infarction
Oxygen (^{17}O)	Oxidative phosphorylation	Calculation of myocardial oxygen consumption

**Figure 1** ^{31}P cardiac spectrum.

upon detecting radiofrequency (RF) signals given off by hydrogen nuclei (protons, ^1H), as their abundance in water and fat allows for a signal to be easily detected from the heart. However, any other nuclei with a magnetic moment, including ^{31}P (Phosphorus (^{31}P)), ^{23}Na (Sodium (^{23}Na)) and ^{13}C (Carbon (^{13}C)) can be detected by MR. The utility of these different elements is summarized in *Table 1*.

When a tissue is placed in a strong magnetic field (referred to as the B_0 field), these nuclei interact with the field, resulting in tissue becoming very weakly magnetised. The nuclei rotate (known as precession or oscillation) at a frequency proportional to the magnetic field. A pulse of RF energy creates additional magnetic field perpendicular to the B_0 field (called B_1), which can tip this magnetisation away from the direction of B_0 (i.e., cause excitation). As the magnetisation relaxes back after excitation, it induces a voltage in a receiver coil which can be detected as a RF signal. This is signal known as a free induction decay (FID), which can be Fourier transformed to produce a spectrum (4).

A basic MRS experiment relies on the principle that the exact resonance frequency of nuclei depends on their chemical environment, causing slight differences

between metabolites: referred to as ‘chemical shift’ (5). A ^{31}P Phosphorus spectrum is a good example of this (*Figure 1*), where the three peaks of phosphorous nuclei within a molecule of ATP resonating at different frequencies are clearly separable and sit apart from the frequency peak produced by the phosphorus nucleus present in PCr. By manipulating the magnetic field gradients, changes in phase or frequency in the signal can be induced which can allow signals from particular tissues to be precisely localised in the body. This is the basis of magnetic resonance imaging but also allows for spectroscopic techniques that isolate individual tissues: in this case, myocardium.

Human MRS is performed on MR scanners with a field strength of 1.5 tesla (T) or 3 T, however increasingly human 7 T systems are becoming available and animal studies are frequently performed at field strengths up to 21 T. Typically, as field strength increases, the separation of the frequencies making up the peaks increases, allowing different peaks to be more easily separated and better quantified. *Figure 2* compares ^{31}P spectra acquired at different field strengths.

Following acquisition, a spectrum must be analysed to quantify the relative proportions of the constituents.

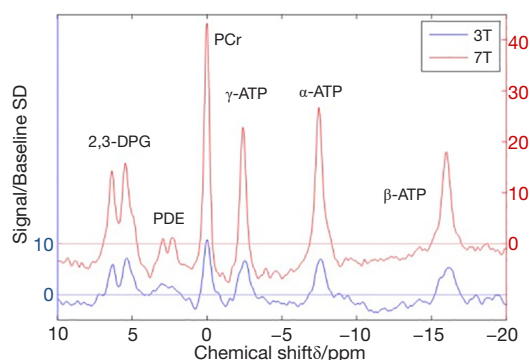


Figure 2 Comparison of cardiac ^{31}P spectra acquired from the same individual at 3 and 7 Tesla field strength. Adapted from (6). 2,3-DPG, 2,3-Diphosphoglycerate; PDE, phosphodiester; ATP, adenosine triphosphate

In comparison to conventional NMR spectroscopy, as used in chemistry, typically *in vivo* MRS spectra have a large number of partially overlapping peaks and therefore are more challenging to quantify. Several automated techniques have been developed for this, either by generating a signal model and fitting it to the data in the time domain, e.g., the Accurate, Robust and Efficient Spectral Fitting (AMARES) technique (7,8). These methods use knowledge of the expected positions of spectral peaks to quantify metabolites in the presence of background noise. It is often necessary to apply correction factors to correct for technical variations in the way that the data acquired and ascertain metabolite concentrations, typically referenced either to an external standard or an internal reference (e.g., water, or ATP).

The heart presents various technical challenges to spectroscopy: it is closely related to other structures that also give off spectral signals: skeletal muscle in the chest wall, the liver lying inferior to the diaphragm and the blood pool flowing through the chambers of the heart. It moves, both with breathing and with the cardiac cycle. The latter can be corrected for with ECG gating (9), breath-holding, respiratory gating with a motion sensor (10) or navigator based motion correction methods (which aim to directly measure diaphragm position with MR) (11), while the former can be ameliorated with pulse sequences that precisely localise signal to a certain portion of the myocardium or methods that apply saturation bands to suppress the unwanted signal from nearby tissues. For these reasons, much MRS has historically been performed prone in order to reduce motion and move the heart slightly closer

to the coil. While increasing B_0 field strength will improve SNR, it also leads to greater inhomogeneities (non-uniformities) within the field, requiring careful technical adjustment of the field to counter the inhomogeneities (known as shimming), a process that is itself complicated by cardiac motion and flow through the heart. Likewise, generating a homogeneous B_1 field is equally important and can be equally difficult.

Cardiac energy metabolism

Energy of hydrolysis of ATP

The energy available from breaking down ATP to ADP and phosphate (P_i) is termed the Gibbs free energy of ATP hydrolysis ($\Delta G'_{\text{ATP hydrolysis}}$ or simply ΔG) and provides a driving force for any ATP requiring reactions within the myocyte. Different reactions require a different ΔG before they can proceed, and the difference between the free energy requirement for the ATPase enzyme and the available free energy from ATP hydrolysis in the local environment can be considered the available driving force or energy reserve for the reaction (12).

The Gibbs free energy of ATP hydrolysis ($\Delta G'_{\text{ATP hydrolysis}}$) can be calculated from the equation (13):

$$\Delta G' = \Delta G^\circ - RT \ln \left(\frac{[\text{ADP}][\text{P}_i]}{[\text{ATP}]} \right) \quad [1]$$

Where ΔG° is the standard free energy change of ATP hydrolysis (-30.5 kJ/mol under standard conditions, where each substrate and product is present at concentration 1 mmol/L , standard temperature and pH 7), R is the ideal gas constant (8.3 J/mol.K) and T is the temperature in kelvin. Note that the ΔG is a negative value and the more negative it is, the more energy is available.

The system can be conceptualised as a water cylinder: the height of the column of water (the ΔG_{ATP}) and how high up each outflow pipe is (the ΔG_{ATP} requirement of that enzyme) will determine the flow into each outflow pipe—i.e., the energy delivered to each ATPase (Figure 3). The myocyte has numerous mechanisms to maintain ΔG_{ATP} at a steady state by coupling production to consumption, however disease states can cause disruption of these processes and a reduction of free energy, disrupting ATP dependent processes (12).

Rises in ADP inhibit the myosin ATPase and their concentration correlates with elevated LV end-diastolic pressure suggesting a link to diastolic dysfunction (14).

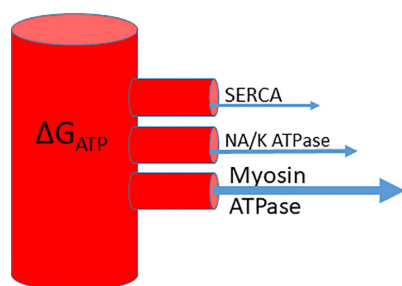


Figure 3 Conception of Delta-G-ATP as a water cylinder exerting pressure.

SERCA (the sarcoplasm-endoplasmic reticulum calcium ATPase or ‘calcium pump’) has the highest ΔG_{ATP} requirement and as the level falls, it loses its ability to maintain the calcium signalling gradient important for contraction and relaxation (15). In experiments involving perfused hearts, when ATP delivery reduces, supply cannot keep up with demand and ADP concentrations increased under stress, resulting in a fall in ΔG_{ATP} . These hearts were unable to increase contractile performance after ΔG_{ATP} had fallen from a normal level of around -58 kJ/mol to nearer -52 kJ/mol (16).

Cardiac substrate metabolism

The normal heart is highly flexible in the fuel it uses as an energetic substrate, which allows natural fluctuations in supply and demand to be accommodated. Normally, the heart metabolises 60–70% fatty acids, with the remainder made up by glucose but which energetic substrate is used can alter dependent upon conditions with feeding, exercise, pressure overload or ischaemia increasing utilisation of glucose (1).

Substrate metabolism in the normal heart

The principal pathways are summarised in *Figure 4*.

GLUT transporters mediate the uptake of glucose into the cell, where it is converted by glycolysis to pyruvate. Pyruvate is taken up into the mitochondria, where it is converted to Acetyl Co-enzyme A for entry into the Krebs cycle. Pyruvate dehydrogenase is the rate limiting enzyme in this pathway: its regulation is complex, being activated by PDH kinases (PDKs) and inactivated by PDH phosphatase, these enzymes in turn being subject to activating and

inactivating forces (17,18).

Fatty acids enter the cardiomyocyte either passively or via a transporter protein such as a Fatty Acid Translocase (FAT or CD36) and then transported into the mitochondrion via esterification to carnitine. Once inside the mitochondrion, the long-chain acyl CoA is oxidised in beta-oxidation to produce Acetyl-CoA, which enters the Krebs cycle (19). Beta oxidation is regulated by the peroxisome proliferator activated receptor (PPAR) family, in particular PPAR- α (20).

Energy of synthesis of ATP

The energy available to produce ATP at the mitochondria is referred to as the energy of synthesis of ATP and is influenced by the type and quantity of metabolic ‘fuel’ used by the mitochondria.

Fat and glucose are metabolised to produce NADH and FADH₂, which donate electrons to the electron transport chain, a series of transmembrane complexes which pump hydrogen ions into the mitochondrial membrane space. These hydrogen ions diffuse back into the mitochondrion via the F₀F₁ ATPase, which produces ATP from ADP and the greater the gradient in chemical potential between inside and outside, the greater the energy of synthesis of ATP (21).

However, each molecule of FADH₂ produces less energy difference between inside and outside the membrane than a molecule of NADH (22) and, as fatty acid oxidation produces more FADH₂ than NADH compared to glucose or ketone, the energy of synthesis will differ depending upon which is metabolised.

Substrate metabolism in the failing heart

Studies of the resting heart in advanced heart failure (dilated cardiomyopathy in humans or experimentally induced heart failure in animal models) show that both fatty acid and glucose uptake and utilisation are reduced (23–27). However, fat uptake is reduced relatively more than glucose so a relative ‘substrate switch’ towards glucose is frequently described (18) and the heart loses its flexibility, becoming more reliant on glucose as a source of energy (28).

However, the increased glucose uptake and glycolysis become decoupled from glucose oxidation, which actually declines (28), leaving the failing heart increasingly reliant on glycolysis with a reduction in fat and glucose oxidation in the mitochondria.

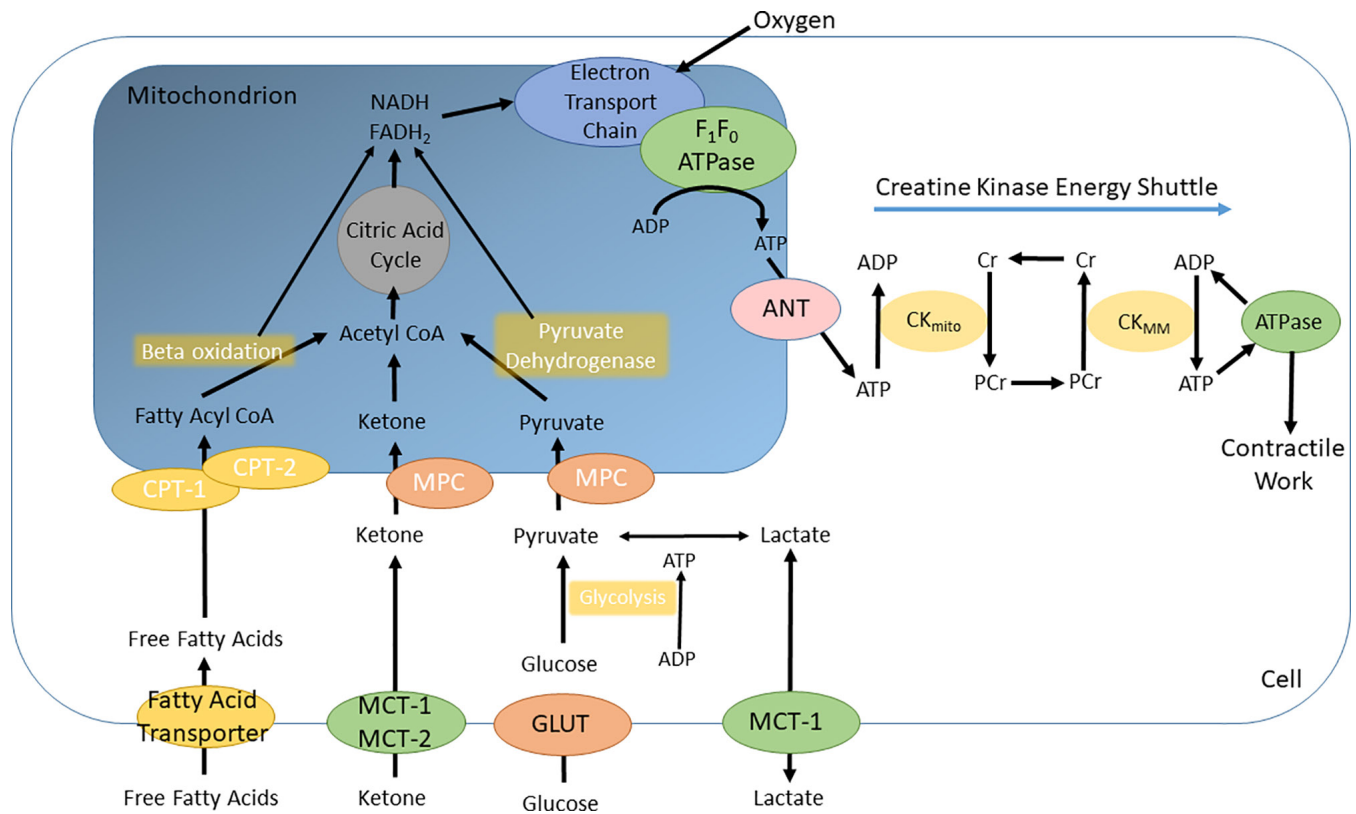


Figure 4 Simplified schematic of substrate metabolism.

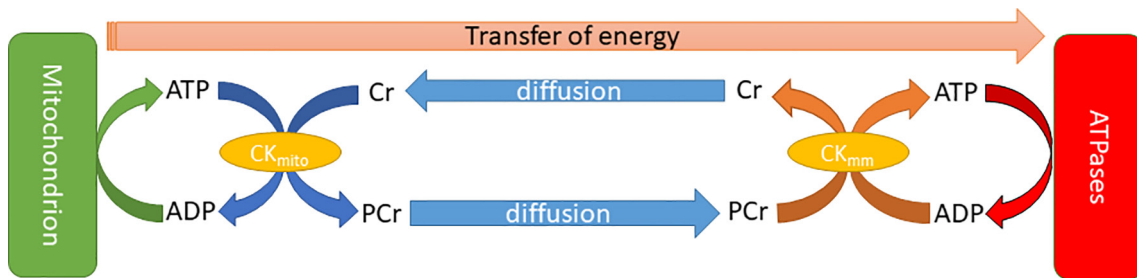
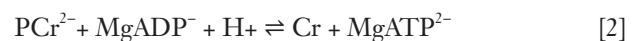


Figure 5 Schematic of energy transfer through the cell.

Phosphotransfer

While ATP is synthesized in the mitochondria, its large size and relative polarity limits the distance it can rapidly diffuse (29), necessitating the evolution of a more transportable “energy carrier”. One of these is phosphocreatine (PCr), produced when ATP’s gamma phosphoryl group is transferred to creatine by the enzyme creatine kinase (CK). Wherever ATP is consumed, this reaction can be reversed to transfer the phosphoryl group

to ADP and re-form ATP. In the heart, PCr is used as the prime temporal and spatial energy reserve: it forms a pool which can buffer short-term changes in demand (30) or supply of ATP and can move around the cell more easily.



See Figure 5.

The equilibria of these reactions are strongly biased to favour the formation of ATP, to the extent that cellular ATP, ADP and Pi concentrations will remain constant except

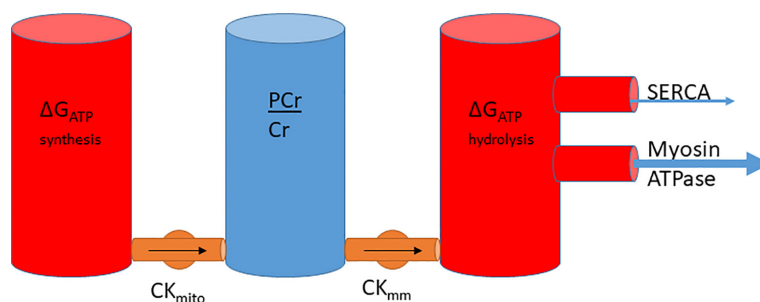


Figure 6 Cylinder concept linking energy of synthesis, phosphocreatine reserves and energy of hydrolysis.

in extreme circumstances, typically preceding cellular death (31). CK carries approximately 80% of intracellular energy flux, with the remainder divided between adenylate kinase (15%) and glycolysis (32).

The energy of synthesis therefore can be linked to energy of hydrolysis, with PCr sitting between both as a transfer network and as a buffer. Extending the cylinder analogy in the previous section, the system can be conceptualised as a series of water cylinders, with flow in or out taking place of production or consumption of ATP, pumping between the cylinders conceptualising CK and the height of water exerting pressure representative of the free energy, ΔG (Figure 6).

Linking supply to demand

The heart has a remarkable ability to match ATP synthesis to hydrolysis with cardiac oxygen consumption, increasing proportionately with workload but intracellular ATP concentrations and ΔG_{ATP} remaining constant (33). In the healthy heart, PCr/ATP remains constant under moderate stress (34,35) suggesting that at these workloads there is sufficient ability to increase substrate metabolism, oxidative phosphorylation and phosphotransfer rates to meet the increased ATP demand. Multiple processes (Calcium levels, AMP signalling, coupled reactions) interact to produce this balance which is thoroughly reviewed by Saks *et al.* (36).

³¹P spectroscopy

Many techniques of varying complexity exist to localise spectral signals from a voxel or region of interest within the myocardium. The simplest is depth resolved surface coil spectroscopy (DRESS) where a single slice parallel to the surface coil is selected by applying a gradient (37). Image selected *in-vivo* spectroscopy (ISIS) selects a single voxel in

three dimensions using inversion pulses applied with MR gradients, but can be very sensitive to respiratory motion. Chemical shift imaging, or CSI uses frequency or phase encoding to differentiate signals from different areas in space. One-dimensional chemical shift imaging (1D-CSI) uses a stepped gradient to encode multiple sections parallel to the coil, acquiring a ‘stack’ of spectra along the axis of the gradient. In 2D or 3D CSI, gradient and phase encoding are used to build up a matrix of individual voxels (38) (Figure 7). While CSI could be considered the method of choice for selecting an area of myocardium, it has downsides: it can lead to very long acquisition times and/or a small matrix size (i.e., a small total number of voxels), and where there is a small number of voxels, each voxel may have contributions from neighbouring tissues (39). In order to sample a non-cuboidal voxel (i.e., a complex three dimensional structure like the heart), methods such as SLOOP (spatial localization with optimal point-spread function) can be employed which remove some of this interference (40).

Cardiac ³¹P spectrum demonstrates the relative proportions of PCr and the three phosphate groups of ATP (Figure 1). At high field strength or in isolated hearts, inorganic phosphate (Pi) and phosphodiester (PDE) may be seen (41), although these are often hard to distinguish from a broad peak created by 2,3-diphosphoglycerate (DPG) from the blood pool. The DPG peak does however allow for contamination in metabolite concentrations from the blood pool to be corrected for.

Relating phosphorous biochemistry to ³¹Phosphorous spectra

In a healthy myocyte, if ATP demand rises, various coupled processes (predominantly calcium but also changes in ADP around the mitochondria) will stimulate more production to meet this demand. However if this energy-producing ability is impaired (most markedly in ischaemic myocardium, but also in

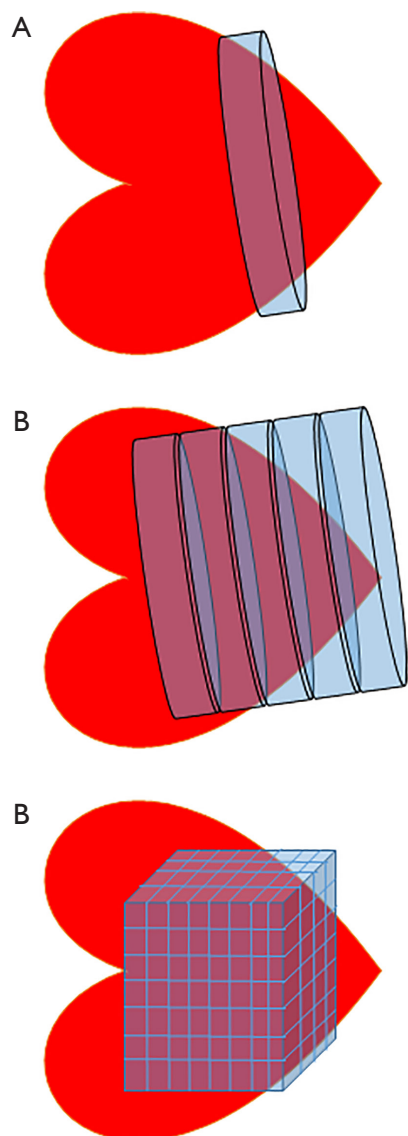


Figure 7 Comparison of spectroscopy techniques. (A) DRESS spectroscopy; (B) 1D CSI; (C) 3D CSI.

diabetes, obesity and heart failure), PCr is depleted to maintain levels of ATP. In fact, levels of ATP only start to fall when PCr is reduced significantly (42). This can be detected via ^{31}P MRS as a change in the ratio between the peak heights of PCr and ATP and expressed mathematically as the PCr/ATP ratio. As ATP levels are kept relatively constant, a fall in PCr/ATP ratio implies a fall in PCr concentration and, knowing that ATP/ADP and PCr/Creatine are in equilibrium, a rise in ADP concentration, reducing ΔG_{ATP} (43).

Absolute quantification of PCr and ATP is more useful than showing the ratio (which assumes that

the concentration of ATP remains constant while the concentration of PCr may vary, driving any changes in the PCr/ATP ratio) but is technically challenging. It can be achieved by using a reference standard with a known concentration outside the chest (44) or by referencing to the tissue proton content, determined by ^1H -MRS (45), although this method is not often used in practice owing to differences in the performance of ^1H and ^{31}P RF coils. Although it has yet to be used in humans, combined ^1H and ^{31}P approaches have been used in animals to measure ADP and calculate ΔG (46).

Saturation transfer techniques are able to quantify the rate of the CK reaction and therefore give an assessment of the rate of transfer of ATP from mitochondria to sites of use as a measure of consumption. These techniques involve using a frequency selective saturation pulse to suppress the signal from the gamma phosphorus group of ATP then measure the reduction in signal as this is transferred into the PCr pool (47).

Finally, ^{31}P -MRS can also be used as a non-invasive tool to measure tissue pH as the chemical shifts of many compounds in the phosphorous spectrum are pH dependent. In a ^{31}P spectrum, the chemical shift of P_i is most sensitive to changes in pH near neutrality. As P_i has a low concentration, high resolution spectra have to be acquired and as it is hidden by the 2,3-DPG peak at low field strength, broadband ^1H decoupling or a high field has to be used. Scanning at 7T ameliorates these issues (41), permitting changes in myocardial pH under stress to be observed using this technique, demonstrating pH reduction with increased lactate production in the anaerobic glycolytic myocardium, for instance during ischaemia.

ATP and heart failure in vivo

Concentrations of ATP and PCr are lower in the failing human heart than in healthy comparators (48-51), however the PCr falls to a much greater extent, and demonstrates into a reduced PCr/ATP ratio.

In heart failure, the total creatine pool is diminished (52) and it has been suggested this protects against a fall in the concentration of PCr, as the ratio of PCr to creatine is maintained and prevents a chemical equilibrium shift to cause a decrease in the ATP/ADP ratio and therefore a less negative (i.e., reduced) ΔG_{ATP} (53). Therefore, it is important to distinguish between changes occurring in minutes versus those occurring over months. In a short term experiment (for instance, comparing the PCr/ATP spectra

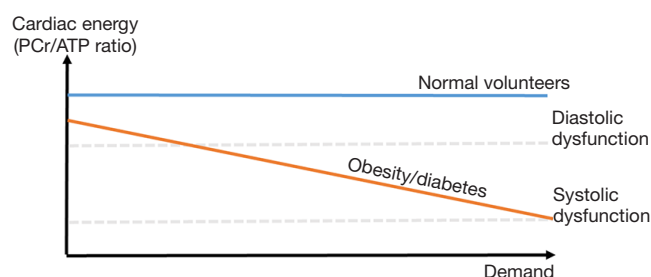


Figure 8 Energy supply outstripping demand in metabolic cardiomyopathies.

of a heart at rest and under stress) the total creatine pool size is unchanged so a decrease in PCr will mean an increase in creatine. Remembering that PCr + ADP and Cr + ATP are in a chemical equilibrium, we can surmise that changes in the balance of PCr/Cr will alter the balance of ATP/ADP and a change in [PCr] will signal a change in the ratio of ATP and ADP and therefore a change in ΔG_{ATP} . Put more simply: when we assume total creatine pool size to remain constant and [ATP] to be maintained in the myocyte, a change in the PCr/ATP ratio must mean a change in [ADP] and thus a change in ΔG_{ATP} .

However, comparing spectra in the longer term (e.g., comparing spectra over the course of evolving heart failure), a fall in total creatine pool size will buffer changes in [PCr] and therefore a fall over months cannot be directly linked to a change in ΔG_{ATP} . In progressive heart failure, both PCr and ATP concentrations fall, so a lowered PCr/ATP ratio in fact reflects a greater decline in PCr than in ATP (54).

PCr/ATP is reduced even in subclinical cardiac dysfunction (25,55-57) and, interestingly, in heart failure with preserved ejection fraction it is correlated with the degree of diastolic impairment (58), drawing a parallel with the linear relationship seen between left ventricular end diastolic pressure and ADP concentration seen in perfused rat hearts (59). A reduction in PCr/ATP predicts mortality in dilated cardiomyopathy (60), correlates with NYHA class (61) and also with left ventricular ejection fraction (62). Changes are also reliably seen in hypertrophic cardiomyopathy (63).

Phosphotransfer, too, is impaired in heart failure, when measured non-invasively via saturation transfer techniques (where it is a predictor of mortality) (64). This may be a more sensitive marker than PCr/ATP ratio, as it quantifies the transfer of phosphate through the system rather than a single measurement which is affected by multiple factors (65).

As many treatments act by reducing energetic demands

upon the heart (by vasodilating or reducing preload), it is not a surprise that some small studies have shown increases in PCr/ATP following treatment (61). As the idea of the heart being energetically starved continues to gain traction, some studies have used PCr/ATP to show benefit in treatments that boost the energetic supply of the heart: the xanthine oxidase inhibitor allopurinol (66) and the carnitine palmitoyl transferase inhibitor perhexiline (67).

A failure to respond to increased supply

As in the resting state, metabolic inflexibility characterises the failing heart. It is unable to increase glucose and fatty acid uptake during rapid pacing stress (23), and remains similar to that seen in the resting state (68). The causes are multifactorial and overlapping with those which impair metabolism in the resting heart.

In response to increased workload, a fall in PCr/ATP on dobutamine stress in obese (55) and diabetic (69) individuals occurs (compared to normal volunteers who exhibited no PCr/ATP fall at similar workloads), demonstrating the role for PCr as a buffer store of high energy phosphate groups when ATP demand exceeds supply. Diastolic dysfunction was also seen to worsen with increasing heart rate (in contrast with the control groups) suggesting progressive failure of the provision of ATP required to maintain $\Delta G'_{ATP}$ for lusitropy (55). This provides evidence that during workloads at which the normal heart can maintain ATP delivery, obese and diabetic hearts cannot (*Figure 8*).

Hyperpolarised ^{13}C spectroscopy

Carbon-13 has a very low natural abundance and low polarity, so on its own gives a poor signal. However, by labelling a compound (e.g., glucose or pyruvate) with ^{13}C , this compound will stand out against the low levels of background ^{13}C present in the myocardium. The technique of hyperpolarisation can boost the signal to noise ratio (SNR) by more than 10,000 times, allowing acquisition of spectra on a second to second basis, allowing the metabolism of the compound to be demonstrated.

To hyperpolarise a sample, the ^{13}C labelled molecule is mixed with a stable radical, placed in a high magnetic field ($>3.35\text{ T}$) and cooled to $<1.4\text{ K}$. At this temperature, the electron spins of the radical are almost completely polarised. Irradiation with microwaves near to the resonant frequency of the electron spin transfers this polarisation to the ^{13}C nuclei. A superheated, pressurised buffer is used to rapidly

melt the molecule, and return it to near room temperature with 30–50% polarisation, which then decays exponentially over the next 2–3 minutes. This rapid decay means there is only a short time to administer the pyruvate to the subject under test and acquire spectra before signal is lost (70).

As the compound is metabolised, different spectral peaks will appear from the new metabolic products. For instance, if pyruvate is labelled in the position of the first carbon (termed [$1\text{-}^{13}\text{C}$]pyruvate) and administered intravenously, over time new peaks of lactate, alanine and bicarbonate will appear as the pyruvate is metabolised to these compounds, allowing quantification of flux through pyruvate dehydrogenase (and therefore glucose oxidation) via rate of production of bicarbonate or anaerobic metabolism via lactate production. Alternatively, labelling in the C2 position means the relevant carbon group passes into acetyl Co-A and then into the Krebs cycle, so this can be used to measure rates of the initial steps in the central Krebs cycle (71). Similarly, labelled butyrate can give insights into fatty acid metabolism (72) and labelled acetoacetate or beta-hydroxybutyrate the metabolism of ketone bodies (73). The technique is flexible enough to permit a variety of other small molecules to be observed, such as acetate, revealing myocardial viability (74), or the conversion of fumarate to malate, which is only detectable in the heart following necrotic cell death (75).

Currently, cell metabolism is clinically studied using positron emission tomography (PET) based techniques, however these have the clinical disadvantage of exposure to radiation and the experimental disadvantage that they show uptake of a metabolite but not its downstream metabolism. As the uptake and oxidation of glucose are distinct entities, this limitation is a significant one. The use of ^{13}C removes both of these obstacles and therefore forms an exciting tool to make novel observations about cardiac metabolism *in vivo* (71).

Applications of hyperpolarised ^{13}C in cardiac studies

Much of this work has so far been performed in animal models, initially looking at ischaemia in isolated heart (76) and intact animals (77). In rat models of hypoxia, it has been used to show an initial shift to lactate production which returned to baseline over 3 weeks (78). Glucose metabolism in diabetes lends itself well to assessment via this technique and it has shown a reduction in pyruvate dehydrogenase flux in the hearts of diabetic mice (79), which was reversible on treatment with dichloroacetate, correlating with a

normalisation of diastolic function (80).

Various heart failure models have been studied. In a porcine pacing model of heart failure, PDH flux monitored by ^{13}C magnetic resonance spectroscopy was maintained until late in the disease process, where it accompanied a transition into dilated cardiomyopathy (25), in Doxorubicin induced cardiomyopathy in rats, PDH flux and Krebs cycle flux were both reduced (81), while in a mouse model of cardiac hypertrophy, maintained levels of PDH flux were shown while lactate production increased, indicating a decoupling of glycolysis (82). Human studies have yet to be undertaken, however there are exciting possibilities. From a research perspective, there is increasing interest in targeting the heart with metabolic treatments and a better understanding of glucose metabolism in different types and stages of heart failure may help unlock novel drug targets. On a clinical level, phenotyping the metabolic changes in individual cases of heart failure might allow better targeting of therapies for an individual patient.

The idea that hyperpolarised imaging could be applied as an imaging modality to show regional lactate production and provide assessment of myocardial viability is an exciting one. The first human cardiac hyperpolarised [$1\text{-}^{13}\text{C}$]pyruvate images were produced by Cunningham in 2016 (83) and hyperpolarised techniques have been used as an imaging biomarker in animal models with pyruvate (84) and fumarate (75).

^1H spectroscopy

Protons are the most abundant of all the MR detectable nuclei, as well as the most sensitive and are contained in essentially all important metabolites: lipids, lactate, creatine, carnitine and taurine (10,85). The disadvantage is that the spectra produced are complex: dominated by a large peak from water (which must be suppressed to make other resonances visible) and many resonances overlap, making them hard to identify. Furthermore, the low endogenous concentrations of most metabolites of interest, typically in the low mM range, makes proton MRS a far harder prospect than the conventional MR imaging of water.

Single voxel sequences such as stimulated echo acquisition mode (STEAM) and point-resolved spectroscopy (PRESS) are widely used and metabolite concentrations are referenced to the water signal, hence spectra are acquired with and without water suppression. CSI can be used to detect regional differences in metabolite concentrations, however a long scan duration limits its utility (86), leading

to the development of accelerated CSI sequences, such as echo-planar spectroscopic imaging (EPSI), which also integrates cardiac triggering and respiratory navigation to produce maps of the spatial distribution of metabolite concentrations within the heart (85).

Myocardial triglyceride and heart failure

Normally, the uptake of fat into the myocyte and its oxidation to produce energy are tightly coupled. However, in some disease states there is a reduction in fatty acid oxidation and accumulation of fats within the cell as tri-acyl glyceride (TAG). For instance, ischaemia, sepsis and heart failure can all reduce oxidation while the excess circulating fats in obesity, diabetes and metabolic syndrome can result in increased uptake (87). This accumulation causes the activation of pro-inflammatory pathways linked with fibrosis and alterations in fatty acid and glucose metabolism that further contribute to myocardial dysfunction (88).

^1H -MRS can quantify myocardial triglyceride levels, which have been shown to predict myocardial strain and energetics in a diabetic population (89), diastolic dysfunction in diabetics (90) and dysfunction in aging men (91). In obesity, myocardial triglyceride determined by ^1H spectroscopy was, along with PCr/ATP ratio, a more important determinant of diastolic function than factors such as degree of hypertrophy which were conventionally thought to be causative (57).

These changes have been shown to be reversible and interestingly, a dietary intervention in type 2 diabetics reduced myocardial triglyceride in association with an improvement in diastolic function (92).

Myocardial creatine quantification

As mentioned above, Creatine is vital for transport of high energy phosphate around the myocyte in the CK system. ^1H -MRS allows quantification of the total creatine pool (i.e., both PCr and free creatine) and, when combined with ^{31}P -MRS this can give a full determination of the quantities of PCr and free Cr, allowing the levels of ADP to be estimated and therefore ΔG calculated.

This technique has been used to confirm histological data showing depletion of the creatine pool in dilated cardiomyopathy (93,94), hypertrophic cardiomyopathy (93,94) and ischaemic heart disease (94). Interestingly, levels of creatine correlated with ejection fraction (93).

^2H spectroscopy

A recent development in spectroscopy has been in using deuterium (^2H) labelling of compounds. Deuterium is also MR visible, but only has 0.0115% natural abundance, hence labelling compounds such as glucose or acetate with ^2H can allow the production of a signal from these compounds only, which allows visualisation of labelled compounds being processed into downstream metabolites in a similar fashion to ^{13}C labelled compounds. Unlike ^1H , ^2H typically has very short relaxation times, which permits the acquisition of signal at thermal equilibrium via multiple averages rapidly. This has been demonstrated in human brain and liver and the opportunities for translation to cardiac uses is an exciting possibility (95).

^{23}Na imaging

Sodium MRI is problematic as it has approximately one 6,000th the signal-to-noise ratio of ^1H and exhibits unusual relaxation behaviour which requires specialised sequences. One useful feature is that intracellular and extracellular relaxation properties are different, which can be enhanced with shift reagents (however none are available for clinical use owing to toxicity) (96).

Nonetheless, sodium's importance in the cardiac action potential and the disruption of sodium currents in various disease states makes it an attractive target for research. Currently, results have only been shown in ischaemia, where loss of ion homeostasis causes intracellular sodium levels to increase while oedema increases the levels of (sodium rich) extra-cellular fluid in tissues. This results in an increase in tissue sodium concentration, which has been demonstrated in humans following MI (97,98) but unfortunately the technique has failed to equal far simpler clinically available measures such as late gadolinium imaging in its sensitivity to detect infarct. More recently, ^{23}Na imaging has been proposed to investigate the linkage between heart and kidney in disease (the cardiorenal syndrome), and combined imaging of these organs has been demonstrated at 7T (99).

^{17}O spectroscopy

Myocardial oxygen consumption is another potential application of MRS by demonstrating turnover of the ^{17}O isotope. The rate of production of H_2^{17}O production in an individual breathing $^{17}\text{O}_2$ enriched air can be tracked (100)

and studies have investigated the feasibility of this technique in animal (101) and human (102) subjects to quantify cardiac myocardial oxygen consumption rate (MVO₂). The low natural abundance of ¹⁷O, the expense in acquiring ¹⁷O labelled compounds, and necessarily long acquisition times have limited the translational applications of this technique.

Other nuclei

Seven tesla MRS has made it feasible to detect other nuclei such as fluorine (¹⁹F), chlorine (³⁵Cl) (103) and potassium (³⁹K) (104). The former does not exist in the body and therefore has potential as a tracer, while the latter two present opportunities for tracking ion flux across membranes.

Future directions

Increasing usage of high-field MRS makes previously technically impossible tasks appear on the horizon, for instance the calculation of energy of hydrolysis of ATP from combined ³¹P and ¹H techniques. Technical improvements in spatial localisation and scan time will continue to increase the utility of MR spectroscopy. Comparative analysis of different areas of myocardium may allow regional differences to be detected, for instance in ischaemia using hyperpolarised ¹³C-MRS to demonstrate lactate production or ³¹P-MRS to show depletion of PCr, while progression in ¹³C-MRS may allow different types of heart failure to be better understood and therapies targeted to produce better outcomes for patients. These techniques may allow MRS to transition from research tool to being a sensitive probe of cellular processes in a clinical investigation.

Acknowledgments

Funding: WD Watson is funded by the British Heart Foundation (Clinical Research Training Fellowship HSR00740). JJJ Miller would like to acknowledge financial support by a Novo Nordisk Postdoctoral Fellowship scheme run in conjunction with the University of Oxford, and also by St Hugh's and Wadham College in the University of Oxford. L Valkovič is funded by the Royal Society and Wellcome Trust (Sir Henry Dale Fellowship #098436/Z/12/B). The support of the Slovak grant agencies APVV (grant #15/0253) and VEGA (grant #2/0003/20) is also gratefully acknowledged.

Footnote

Provenance and Peer Review: This article was commissioned by the Guest Editors (Oliver Rider and Andrew J. Lewis) for the series “The use of advanced cardiac MRI in heart failure and cardiac hypertrophy” published in *Cardiovascular Diagnosis and Therapy*. The article was sent for external peer review organized by the Guest Editors and the editorial office.

Conflicts of Interest: All authors have completed the ICMJE uniform disclosure form (available at <http://dx.doi.org/10.21037/cdt.2019.12.13>). The series “The Use of Advanced Cardiac MRI in Heart Failure and Cardiac Hypertrophy” was commissioned by the editorial office without any funding or sponsorship. AL and OJR served as the unpaid Guest Editors of the series. JJJM reports grants from Novo Nordisk, during the conduct of the study; In addition, JJJM has a patent Radiofrequency Coil, GB1905844.5 pending. AL reports other from Bayer, personal fees from Boehringer Ingelheim, outside the submitted work; SN reports grants from Boehringer Ingelheim, grants from Cytokinetics, personal fees from P zer, personal fees from Cytokinetics, outside the submitted work. The authors have no other conflicts of interest to declare.

Ethical Statement: The authors are accountable for all aspects of the work in ensuring that questions related to the accuracy or integrity of any part of the work are appropriately investigated and resolved.

Open Access Statement: This is an Open Access article distributed in accordance with the Creative Commons Attribution-NonCommercial-NoDerivs 4.0 International License (CC BY-NC-ND 4.0), which permits the non-commercial replication and distribution of the article with the strict proviso that no changes or edits are made and the original work is properly cited (including links to both the formal publication through the relevant DOI and the license). See: <https://creativecommons.org/licenses/by-nc-nd/4.0/>.

References

1. Stanley WC, Recchia FA, Lopaschuk GD. Myocardial substrate metabolism in the normal and failing heart. *Physiol Rev* 2005;85:1093-129.
2. Renguet E, Bultot L, Beauloye C, et al. The Regulation of

- Insulin-Stimulated Cardiac Glucose Transport via Protein Acetylation. *Front Cardiovasc Med* 2018;5:70.
3. Neubauer S. The failing heart - an engine out of fuel. *N Engl J Med* 2007;356:1140-51.
 4. Balaban RS, Peters DC. Basic Principles of Cardiovascular Magnetic Resonance. In: Manning WJ, Pennell DJ, editors. *Cardiovascular Magnetic Resonance: A Companion to Braunwald's Heart Disease*. 3rd edition. Philadelphia, PA: Elsevier, 2019:1-14.
 5. Holloway CJ, Suttie J, Dass S, et al. Clinical cardiac magnetic resonance spectroscopy. *Prog Cardiovasc Dis* 2011;54:320-7.
 6. Rodgers CT, Clarke WT, Snyder C, et al. Human cardiac 31P magnetic resonance spectroscopy at 7 Tesla. *Magn Reson Med* 2014;72:304-15.
 7. Vanhamme L, van den Boogaart A, Van Huffel S. Improved method for accurate and efficient quantification of MRS data with use of prior knowledge. *J Magn Reson* 1997;129:35-43.
 8. Purvis LAB, Clarke WT, Biasioli L, et al. OXSA: An open-source magnetic resonance spectroscopy analysis toolbox in MATLAB. *PLoS One* 2017;12:e0185356.
 9. Lanzer P, Barta C, Botvinick EH, et al. ECG-synchronized cardiac MR imaging: method and evaluation. *Radiology* 1985;155:681-6.
 10. Szczepaniak LS, Dobbins RL, Metzger GJ, et al. Myocardial triglycerides and systolic function in humans: In vivo evaluation by localized proton spectroscopy and cardiac imaging. *Magn Reson Med* 2003;49:417-23.
 11. Kozerke S, Schär M, Lamb HJ, et al. Volume tracking cardiac 31P spectroscopy. *Magn Reson Med* 2002;48:380-4.
 12. Ingwall JS. *ATP and the Heart*. Boston: Kluwer Academic Publishers, 2002.
 13. Veech RL. The determination of the redox states and phosphorylation potential in living tissues and their relationship to metabolic control of disease phenotypes. *Biochem Mol Biol Educ* 2006;34:168-79.
 14. Tian R, Christe ME, Spindler M, et al. Role of MgADP in the development of diastolic dysfunction in the intact beating rat heart. *J Clin Invest* 1997;99:745-51.
 15. Chen W, London R, Murphy E, et al. Regulation of the Ca²⁺ gradient across the sarcoplasmic reticulum in perfused rabbit heart. A 19F nuclear magnetic resonance study. *Circ Res* 1998;83:898-907.
 16. Tian R, Ingwall JS. Energetic basis for reduced contractile reserve in isolated rat hearts. *Am J Physiol* 1996;270:H1207-16.
 17. Sheeran FL, Pepe S. Mitochondrial Bioenergetics and Dysfunction in Failing Heart. *Adv Exp Med Biol* 2017;982:65-80.
 18. Peterzan MA, Lygate CA, Neubauer S, et al. Metabolic remodeling in hypertrophied and failing myocardium: a review. *Am J Physiol Heart Circ Physiol* 2017;313:H597-616.
 19. Ritterhoff J, Tian R. Metabolism in cardiomyopathy: every substrate matters. *Cardiovasc Res* 2017;113:411-21.
 20. Noordali H, Loudon BL, Frenneaux MP, et al. Cardiac metabolism - A promising therapeutic target for heart failure. *Pharmacol Ther* 2018;182:95-114.
 21. Mitchell PD. *Chemiosmotic coupling and energy transduction*. Glynn Research; 1968.
 22. Veech RL. The therapeutic implications of ketone bodies: the effects of ketone bodies in pathological conditions: ketosis, ketogenic diet, redox states, insulin resistance, and mitochondrial metabolism. *Prostaglandins Leukot Essent Fatty Acids* 2004;70:309-19.
 23. Neglia D, De Caterina A, Marraccini P, et al. Impaired myocardial metabolic reserve and substrate selection flexibility during stress in patients with idiopathic dilated cardiomyopathy. *Am J Physiol Heart Circ Physiol* 2007;293:H3270-8.
 24. Brown DA, Perry JB, Allen ME, et al. Expert consensus document: Mitochondrial function as a therapeutic target in heart failure. *Nat Rev Cardiol* 2017;14:238-50.
 25. Schroeder MA, Lau AZ, Chen AP, et al. Hyperpolarized (¹³C) magnetic resonance reveals early- and late-onset changes to in vivo pyruvate metabolism in the failing heart. *Eur J Heart Fail* 2013;15:130-40.
 26. Zhang L, Jaswal JS, Ussher JR, et al. Cardiac insulin-resistance and decreased mitochondrial energy production precede the development of systolic heart failure after pressure-overload hypertrophy. *Circ Heart Fail* 2013;6:1039-48.
 27. Shibayama J, Yuzyuk TN, Cox J, et al. Metabolic remodeling in moderate synchronous versus dyssynchronous pacing-induced heart failure: integrated metabolomics and proteomics study. *PLoS One* 2015;10:e0118974.
 28. Karwi QG, Uddin GM, Ho KL, et al. Loss of Metabolic Flexibility in the Failing Heart. *Front Cardiovasc Med* 2018;5:68.
 29. Dzeja PP, Terzic A. Phosphotransfer networks and cellular energetics. *J Exp Biol* 2003;206:2039-47.
 30. Honda H, Tanaka K, Akita N, et al. Cyclical changes in high-energy phosphates during the cardiac cycle by pacing-Gated 31P nuclear magnetic resonance. *Circ J*

- 2002;66:80-6.
31. Cain DF, Davies RE. Breakdown of adenosine triphosphate during a single contraction of working muscle. *Biochem Biophys Res Commun* 1962;8:361-6.
 32. Pucar D, Dzeja PP, Bast P, et al. Cellular energetics in the preconditioned state: protective role for phosphotransfer reactions captured by 18O-assisted 31P NMR. *J Biol Chem* 2001;276:44812-9.
 33. Balaban RS, Kantor HL, Katz LA, et al. Relation between work and phosphate metabolite in the in vivo paced mammalian heart. *Science* 1986;232:1121-3.
 34. Naumova AV, Weiss RG, Chacko VP. Regulation of murine myocardial energy metabolism during adrenergic stress studied by in vivo 31P NMR spectroscopy. *Am J Physiol Heart Circ Physiol* 2003;285:H1976-9.
 35. Schaefer S, Schwartz GG, Steinman SK, et al. Metabolic response of the human heart to inotropic stimulation: in vivo phosphorus-31 studies of normal and cardiomyopathic myocardium. *Magn Reson Med* 1992;25:260-72.
 36. Saks V, Favier R, Guzun R, et al. Molecular system bioenergetics: regulation of substrate supply in response to heart energy demands. *J Physiol* 2006;577:769-77.
 37. Bottomley PA, Foster TB, Darrow RD. Depth-resolved surface-coil spectroscopy (DRESS) for in Vivo 1H, 31P, and 13C NMR. *J Magn Reson (1969)* 1984;59:338-42.
 38. Bottomley PA. MR spectroscopy of the human heart: the status and the challenges. *Radiology* 1994;191:593-612.
 39. von Kienlin M, Beer M, Greiser A, et al. Advances in human cardiac 31P-MR spectroscopy: SLOOP and clinical applications. *J Magn Reson Imaging* 2001;13:521-7.
 40. von Kienlin M, Mejia R. Spectral localization with optimal pointspread function. *J Magn Reson (1969)* 1991;94:268-87.
 41. Valkovič L, Clarke WT, Schmid AI, et al. Measuring inorganic phosphate and intracellular pH in the healthy and hypertrophic cardiomyopathy hearts by in vivo 7T 31P-cardiovascular magnetic resonance spectroscopy. *J Cardiovasc Magn Reson* 2019;21:19.
 42. Clarke K, O'Connor AJ, Willis RJ. Temporal relation between energy metabolism and myocardial function during ischemia and reperfusion. *Am J Physiol* 1987;253:H412-21.
 43. Weiss RG, Gerstenblith G, Bottomley PA. ATP flux through creatine kinase in the normal, stressed, and failing human heart. *Proc Natl Acad Sci U S A* 2005;102:808-13.
 44. Bottomley PA, Hardy CJ, Roemer PB. Phosphate metabolite imaging and concentration measurements in human heart by nuclear magnetic resonance. *Magn Reson Med* 1990;14:425-34.
 45. Bottomley PA, Atalar E, Weiss RG. Human cardiac high-energy phosphate metabolite concentrations by 1D-resolved NMR spectroscopy. *Magn Reson Med* 1996;35:664-70.
 46. Bottomley PA, Weiss RG. Noninvasive Localized MR Quantification of Creatine Kinase Metabolites in Normal and Infarcted Canine Myocardium. *Radiology* 2001;219:411-8.
 47. Schar M, El-Sharkawy AMM, Weiss RG, et al. Triple Repetition Time Saturation Transfer (TRiST) (31P) Spectroscopy for Measuring Human Creatine Kinase Reaction Kinetics. *Magn Reson Med* 2010;63:1493-501.
 48. Starling RC, Hammer DE, Altschuld RA. Human myocardial ATP content and in vivo contractile function. *Mol Cell Biochem* 1998;180:171-7.
 49. Beer M, Seyfarth T, Sandstede J, et al. Absolute concentrations of high-energy phosphate metabolites in normal, hypertrophied, and failing human myocardium measured noninvasively with (31)P-SLOOP magnetic resonance spectroscopy. *J Am Coll Cardiol* 2002;40:1267-74.
 50. Hardy CJ, Weiss RG, Bottomley PA, et al. Altered myocardial high-energy phosphate metabolites in patients with dilated cardiomyopathy. *Am Heart J* 1991;122:795-801.
 51. Conway MA, Allis J, Ouwerkerk R, et al. Detection of low phosphocreatine to ATP ratio in failing hypertrophied human myocardium by 31P magnetic resonance spectroscopy. *Lancet* 1991;338:973-6.
 52. Zervou S, Whittington HJ, Russell AJ, et al. Augmentation of Creatine in the Heart. *Mini Rev Med Chem* 2016;16:19-28.
 53. Shen W, Vatner DE, Vatner SF, et al. Progressive loss of creatine maintains a near normal DeltaG approximately (ATP) in transgenic mouse hearts with cardiomyopathy caused by overexpressing Galpha. *J Mol Cell Cardiol* 2010;48:591-9.
 54. Ingwall JS. Energy metabolism in heart failure and remodelling. *Cardiovasc Res* 2009;81:412-9.
 55. Rider OJ, Francis JM, Ali MK, et al. Effects of catecholamine stress on diastolic function and myocardial energetics in obesity. *Circulation* 2012;125:1511-9.
 56. Willis BC, Salazar-Cantu A, Silva-Platas C, et al. Impaired oxidative metabolism and calcium mishandling underlie cardiac dysfunction in a rat model of post-acute isoproterenol-induced cardiomyopathy. *Am J Physiol Heart Circ Physiol* 2015;308:H467-77.
 57. Rayner JJ, Banerjee R, Holloway CJ, et al. The relative

- contribution of metabolic and structural abnormalities to diastolic dysfunction in obesity. *Int J Obes (Lond)* 2018;42:441-7.
58. Phan TT, Abozguia K, Nallur Shivu G, et al. Heart failure with preserved ejection fraction is characterized by dynamic impairment of active relaxation and contraction of the left ventricle on exercise and associated with myocardial energy deficiency. *J Am Coll Cardiol* 2009;54:402-9.
 59. Tian R, Nascimben L, Ingwall JS, et al. Failure to maintain a low ADP concentration impairs diastolic function in hypertrophied rat hearts. *Circulation* 1997;96:1313-9.
 60. Neubauer S, Horn M, Cramer M, et al. Myocardial Phosphocreatine-to-ATP Ratio Is a Predictor of Mortality in Patients With Dilated Cardiomyopathy. *Circulation* 1997;96:2190-6.
 61. Neubauer S, Krahe T, Schindler R, et al. ³¹P magnetic resonance spectroscopy in dilated cardiomyopathy and coronary artery disease. Altered cardiac high-energy phosphate metabolism in heart failure. *Circulation* 1992;86:1810-8.
 62. Neubauer S, Horn M, Pabst T, et al. Contributions of ³¹P-magnetic resonance spectroscopy to the understanding of dilated heart muscle disease. *Eur Heart J* 1995;16 Suppl O:115-8.
 63. Shivu GN, Abozguia K, Phan TT, et al. (³¹P) magnetic resonance spectroscopy to measure in vivo cardiac energetics in normal myocardium and hypertrophic cardiomyopathy: Experiences at 3T. *Eur J Radiol* 2010;73:255-9.
 64. Bottomley PA, Panjra GS, Lai S, et al. Metabolic rates of ATP transfer through creatine kinase (CK Flux) predict clinical heart failure events and death. *Sci Transl Med* 2013;5:215re3.
 65. Lygate CA, Neubauer S. Metabolic flux as a predictor of heart failure prognosis. *Circ Res* 2014;114:1228-30.
 66. Hirsch GA, Bottomley PA, Gerstenblith G, et al. Allopurinol acutely increases adenosine triphosphate energy delivery in failing human hearts. *J Am Coll Cardiol* 2012;59:802-8.
 67. Beadle RM, Williams LK, Kuehl M, et al. Improvement in cardiac energetics by perhexiline in heart failure due to dilated cardiomyopathy. *JACC Heart Fail* 2015;3:202-11.
 68. Trico D, Baldi S, Frascerra S, et al. Abnormal Glucose Tolerance Is Associated with a Reduced Myocardial Metabolic Flexibility in Patients with Dilated Cardiomyopathy. *J Diabetes Res* 2016;2016:3906425.
 69. Levelt E, Rodgers CT, Clarke WT, et al. Cardiac energetics, oxygenation, and perfusion during increased workload in patients with type 2 diabetes mellitus. *Eur Heart J* 2016;37:3461-9.
 70. Timm KN, Miller JJ, Henry JA, Tyler DJ. Cardiac applications of hyperpolarised magnetic resonance. *Prog Nucl Magn Reson Spectrosc* 2018;106-107:66-87.
 71. Apps A, Lau J, Peterzan M, et al. Hyperpolarised magnetic resonance for in vivo real-time metabolic imaging. *Heart* 2018;104:1484-91.
 72. Ball DR, Rowlands B, Dodd MS, et al. Hyperpolarized butyrate: a metabolic probe of short chain fatty acid metabolism in the heart. *Magn Reson Med* 2014;71:1663-9.
 73. Miller JJ, Ball DR, Lau AZ, et al. Hyperpolarized ketone body metabolism in the rat heart. *NMR Biomed* 2018;31:e3912.
 74. Koellisch U, Gringeri CV, Rancan G, et al. Metabolic imaging of hyperpolarized [1-(¹³C)]acetate and [1-(¹³C)]acetylcarnitine - investigation of the influence of dobutamine induced stress. *Magn Reson Med* 2015;74:1011-8.
 75. Miller JJ, Lau AZ, Nielsen PM, et al. Hyperpolarized [1,4-¹³C₂]Fumarate Enables Magnetic Resonance-Based Imaging of Myocardial Necrosis. *JACC Cardiovasc Imaging* 2018;11:1594-606.
 76. Schroeder MA, Atherton HJ, Ball DR, et al. Real-time assessment of Krebs cycle metabolism using hyperpolarized ¹³C magnetic resonance spectroscopy. *FASEB J* 2009;23:2529-38.
 77. Aquaro GD, Frijia F, Positano V, et al. 3D CMR mapping of metabolism by hyperpolarized ¹³C-pyruvate in ischemia-reperfusion. *JACC Cardiovasc Imaging* 2013;6:743-4.
 78. Le Page LM, Rider OJ, Lewis AJ, et al. Assessing the effect of hypoxia on cardiac metabolism using hyperpolarized (¹³C) magnetic resonance spectroscopy. *NMR Biomed* 2019;32:e4099.
 79. Le Page LM, Ball DR, Ball V, et al. Simultaneous in vivo assessment of cardiac and hepatic metabolism in the diabetic rat using hyperpolarized MRS. *NMR Biomed* 2016;29:1759-67.
 80. Le Page LM, Rider OJ, Lewis AJ, et al. Increasing Pyruvate Dehydrogenase Flux as a Treatment for Diabetic Cardiomyopathy: A Combined ¹³C Hyperpolarized Magnetic Resonance and Echocardiography Study. *Diabetes* 2015;64:2735-43.
 81. Timm KN, Perera CA, Ball V, et al. Investigating real-time metabolic flux changes in a rat model of doxorubicin-induced cardiotoxicity using hyperpolarized ¹³C magnetic

- resonance spectroscopy. *J Mol Cell Cardiol* 2018;120:34.
82. Seymour AM, Giles L, Ball V, et al. In vivo assessment of cardiac metabolism and function in the abdominal aortic banding model of compensated cardiac hypertrophy. *Cardiovasc Res* 2015;106:249-60.
 83. Cunningham CH, Lau JY, Chen AP, et al. Hyperpolarized ¹³C Metabolic MRI of the Human Heart: Initial Experience. *Circ Res* 2016;119:1177-82.
 84. Ball DR, Cruickshank R, Carr CA, et al. Metabolic imaging of acute and chronic infarction in the perfused rat heart using hyperpolarised [1-¹³C]pyruvate. *NMR Biomed* 2013;26:1441-50.
 85. Weiss K, Martini N, Boesiger P, et al. Metabolic MR imaging of regional triglyceride and creatine content in the human heart. *Magn Reson Med* 2012;68:1696-704.
 86. van Ewijk PA, Schrauwen-Hinderling VB, Bekkers SC, et al. MRS: a noninvasive window into cardiac metabolism. *NMR Biomed* 2015;28:747-66.
 87. Schulze PC, Drosatos K, Goldberg IJ. Lipid Use and Misuse by the Heart. *Circ Res* 2016;118:1736-51.
 88. Sharma S, Adrogoe JV, Golfman L, et al. Intramyocardial lipid accumulation in the failing human heart resembles the lipotoxic rat heart. *FASEB J* 2004;18:1692-700.
 89. Levelt E, Mahmood M, Piechnik SK, et al. Relationship Between Left Ventricular Structural and Metabolic Remodeling in Type 2 Diabetes. *Diabetes* 2016;65:44-52.
 90. Rijzewijk LJ, van der Meer RW, Smit JW, et al. Myocardial steatosis is an independent predictor of diastolic dysfunction in type 2 diabetes mellitus. *J Am Coll Cardiol* 2008;52:1793-9.
 91. van der Meer RW, Rijzewijk LJ, Diamant M, et al. The ageing male heart: myocardial triglyceride content as independent predictor of diastolic function. *Eur Heart J* 2008;29:1516-22.
 92. Hammer S, Snel M, Lamb HJ, et al. Prolonged caloric restriction in obese patients with type 2 diabetes mellitus decreases myocardial triglyceride content and improves myocardial function. *J Am Coll Cardiol* 2008;52:1006-12.
 93. Nakae I, Mitsunami K, Omura T, et al. Proton magnetic resonance spectroscopy can detect creatine depletion associated with the progression of heart failure in cardiomyopathy. *J Am Coll Cardiol* 2003;42:1587-93.
 94. Nakae I, Mitsunami K, Yoshino T, et al. Clinical features of myocardial triglyceride in different types of cardiomyopathy assessed by proton magnetic resonance spectroscopy: comparison with myocardial creatine. *J Card Fail* 2010;16:812-22.
 95. De Feyter HM, Behar KL, Corbin ZA, et al. Deuterium metabolic imaging (DMI) for MRI-based 3D mapping of metabolism in vivo. *Sci Adv* 2018;4:eaat7314.
 96. Bottomley PA. Sodium MRI in human heart: a review. *NMR Biomed* 2016;29:187-96.
 97. Ouwerkerk R, Bottomley PA, Solaiyappan M, et al. Tissue sodium concentration in myocardial infarction in humans: a quantitative ²³Na MR imaging study. *Radiology* 2008;248:88-96.
 98. Sandstede JJ, Pabst T, Beer M, et al. Assessment of myocardial infarction in humans with (²³)Na MR imaging: comparison with cine MR imaging and delayed contrast enhancement. *Radiology* 2001;221:222-8.
 99. Boehmert L, Kuehne A, Waiczies H, et al. Cardiac sodium MRI at 7.0 Tesla using a 4/4 channel ¹H/²³Na radiofrequency antenna array. *Magn Reson Med* 2019;82:2343-56.
 100. Zhu XH, Chen W. In vivo oxygen-17 NMR for imaging brain oxygen metabolism at high field. *Prog Nucl Magn Reson Spectrosc* 2011;59:319-35.
 101. McCommis KS, He X, Abendschein DR, et al. Cardiac ¹⁷O MRI: toward direct quantification of myocardial oxygen consumption. *Magn Reson Med* 2010;63:1442-7.
 102. Borowiak R, Groebner J, Haas M, et al. Direct cerebral and cardiac ¹⁷O-MRI at 3 Tesla: initial results at natural abundance. *Magma* 2014;27:95-9.
 103. Nagel AM, Lehmann-Horn F, Weber MA, et al. In vivo ³⁵Cl MR imaging in humans: a feasibility study. *Radiology* 2014;271:585-95.
 104. Umatham R, Rosler MB, Nagel AM. In vivo ³⁹K MR imaging of human muscle and brain. *Radiology* 2013;269:569-76.

Cite this article as: Watson WD, Miller JJJ, Lewis A, Neubauer S, Tyler D, Rider OJ, Valkovič L. Use of cardiac magnetic resonance to detect changes in metabolism in heart failure. *Cardiovasc Diagn Ther* 2020;10(3):583-597. doi: 10.21037/cdt.2019.12.13